

Excitonic photoluminescence characteristics of amorphous silicon nanoparticles embedded in silicon nitride film

W. Yu^a, J.Y. Zhang, W.G. Ding, and G.S. Fu

College of Physics Science and Technology, Hebei University, Baoding 071002, P.R. China

Received 30 November 2006 / Received in final form 18 April 2007

Published online 25 May 2007 – © EDP Sciences, Società Italiana di Fisica, Springer-Verlag 2007

Abstract. We have investigated the photoluminescence (PL) properties of amorphous silicon nanoparticles (a-Si NPs) embedded in silicon nitride film (Si-in-SiN_x) grown by helicon wave plasma-enhanced chemical vapor deposition (HWP-CVD) technique. The PL spectrum of the film exhibits a broad band constituted of two Gaussian components. From photoluminescence excitation (PLE) measurements, it is elucidated that the two PL bands are associated with the a-Si NPs and the silicon nitride matrix surrounding a-Si NPs, respectively. The existence of Stokes shift between PL and absorption edge indicates that radiative recombination of carriers occurs in the states at the surface of the Si NPs, whereas their generation takes place in the a-Si NPs cores and the silicon nitride matrix, respectively. The visible PL of the film originates from the radiative recombination of excitons trapped in the surface states. At decreasing excitation energy (E_{ex}), the PL peak energy was found to be redshifted, accompanied by a narrowing of the bandwidth. These results are explained by surface exciton recombination model taking into account there existing a size distribution of a-Si NPs in the silicon nitride matrix.

PACS. 78.67.-n Optical properties of low-dimensional, mesoscopic, and nanoscale materials and structures – 71.20.Nr Semiconductor compounds – 78.55.-m Photoluminescence, properties and materials

1 Introduction

Bulk silicon, as the main semiconductor material in microelectronic integrated circuitry, is generally considered to be unsuitable for optoelectronic applications because of its indirect band-gap nature. The discovery of intense visible luminescence in porous silicon at room temperature has greatly stimulated the interest in investigation of the light emission properties of different kinds of silicon-based nanostructures [1–6], motivated by the urgent need of efficient light-emitting materials for optoelectronic and display applications. Particularly, the low-dimensional composite nanostructures, which consist of silicon nanoparticles (Si NPs) embedded in wide-gap silicon compounds such as silicon oxide and silicon nitride, have drawn much attention due to their property of providing robust, well-passivated Si NPs compound films which are compatible with the standard silicon processing technologies. Silicon nitride has a band gap (5.3 eV) that is smaller than that of silicon oxide (9.2 eV), profitable to carrier injection in its optoelectronic application. In addition, there is a short lifetime of about nanosecond for the light emission from Si NPs in silicon nitride film (Si-in-SiN_x) [7], which opens up the possibility of fabricating silicon-based fast optoelec-

tronic devices such as gigahertz optical interconnections. Therefore, the synthesis and optical properties of Si-in-SiN_x composite structure have been extensively studied in recent years.

By now, efficient photoluminescence (PL) across the whole visible light range and beyond has been realized in Si-in-SiN_x films by adjusting the size of Si NPs [7–9]. The origin of such luminescence is often ascribed to the quantum confinement effect of Si NPs in the amorphous matrix [9]. However, there is increasing evidence that the surface passivation and chemical surroundings of Si NPs play a crucial role, not only in reducing nonradiative processes and thus enhancing PL efficiency, but also in taking part in the luminescent processes, which make the PL behavior of compound system more complicated. Therefore, the underlying light emission mechanism of the composite structure is not yet completely understood.

In this work, we have investigated the light emission features of Si-in-SiN_x compound film in order to clarify the luminescence mechanism of the composite structure. Spectral analyses suggest that the radiative recombination of carriers occurs in the states at the surface of the Si NPs, whereas their generation takes place in the Si NPs cores and the silicon nitride matrix, respectively. The influences of surface states on the light emission properties of the Si NPs composite structure are discussed.

^a e-mail: yuwei@hbu.edu.cn

2 Experimental

The Si-in-SiN_x films were prepared by HWP-CVD technique with SiH₄, H₂ and Ar-diluted 6.25% N₂ as the reactant gas sources. The equipment adopted has been described in detail elsewhere [10]. The films were deposited on *n*-type Si (100) wafers and quartz about 2 h. The SiH₄, N₂ and H₂ flow rates were kept at 0.5, 0.5 and 40 sccm, respectively. The total pressure was maintained at 0.5 Pa and the deposition temperature was fixed at 300 °C. The microstructure of a-Si NPs embedded in silicon nitride matrix has been confirmed by transmission electron microscopy (TEM) measurement. The nitrogen content and local bonding configurations of the films have been identified by X-ray photoelectron spectroscopy (XPS) and Raman spectroscopy analysis [11]. The PL spectrum was excited using the 325 nm (3.82 eV) line of a He-Cd laser. The PL spectra at different excitation energies (E_{ex}) and PL excitation (PLE) spectra were excited by the monochromatic light from a 150 W Xe lamp through a monochromator and detected by another monochromator equipped with a photomultiplier. The optical absorption of the film was deduced from ultraviolet-visible transmittance-reflectance measurements. All spectra were corrected for the system response.

3 Results and discussion

Figure 1 shows the PL spectrum of the sample deposited on silicon substrate taken under excitation with the 325 nm (3.82 eV) line of a He-Cd laser at room temperature. The PL intensity is strong enough that can be seen in green by naked eyes. The PL spectrum exhibits a broad band around 2.50 eV which can be well fitted by two Gaussian components. The main band with larger peak intensity is around 2.45 eV with a broad full width at half maximum (FWHM) of 0.56 eV, while the other one with smaller peak intensity peaks at 2.90 eV with a narrower FWHM of 0.43 eV. The integrated area ratio of two Gaussian components is 4.3 to 1. Such a result may imply that the presence of two different processes responsible for PL of the compound film.

To identify the origins of above two components, the PLE spectra monitored at every band peak have been measured. The corresponding PLE spectrum monitored at 2.90 eV is shown in Figure 2. It can be seen that the PLE spectrum shows two excitation bands at around 3.75 and 4.50 eV, respectively. The 4.50 eV PLE peak has relatively larger intensity and broader width. When we take the 276 nm (4.50 eV) line of a Xe lamp as the excitation source, a broad PL band at around 2.85 eV is clearly observed, corresponding to the Gaussian component peaked at 2.90 eV, as shown in the inset of Figure 2. These observations strongly suggest that the excitation band around 4.50 eV is responsible for the PL band around 2.90 eV, while the smaller band at around 3.75 eV may be associated with the PL band around 2.50 eV. For silicon nitride and silicon oxynitride films, previous investigations have indicated that the emission band around 2.6–2.9 eV comes

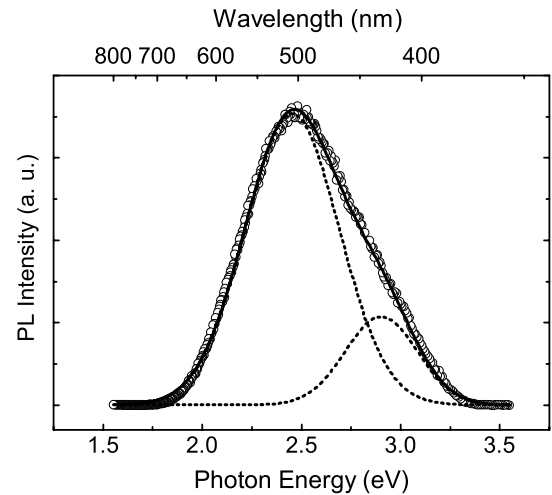


Fig. 1. PL spectrum of the sample taken under excitation with the 325 nm line of a He-Cd laser. Lines denote the fitted results by two Gaussian components.

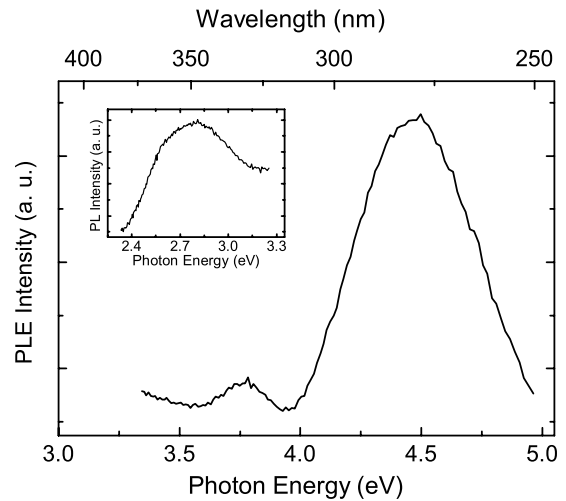


Fig. 2. PLE spectrum of the sample monitored at 2.90 eV. The inset shows the PL spectrum under excitation with the 276 nm line of a Xe lamp.

from the Si–N bonds [12]. The reported PLE peak monitored at 2.40 eV for the PL of hydrogenated silicon nitride film is larger than 4.50 eV [13], similar to the value of second peak obtained in Figure 2. Therefore, we can conclude that the dominant excitation band around 4.50 eV in Figure 2 is due to the interband excitation of the silicon nitride matrix. Considering the existence of large Stokes shift between the PL and excitation band, it is reasonable to assume that the generation of carriers mainly takes place in the extended state, while the radiative recombination occurs after the carriers are trapped into the band tail state.

Figure 3 shows the PLE spectrum of the sample monitored at 2.50 eV. This spectrum exhibits two well-resolved excitation bands peaked at 3.50 and 4.30 eV, respectively. The excitation band around 3.50 eV can be attributed

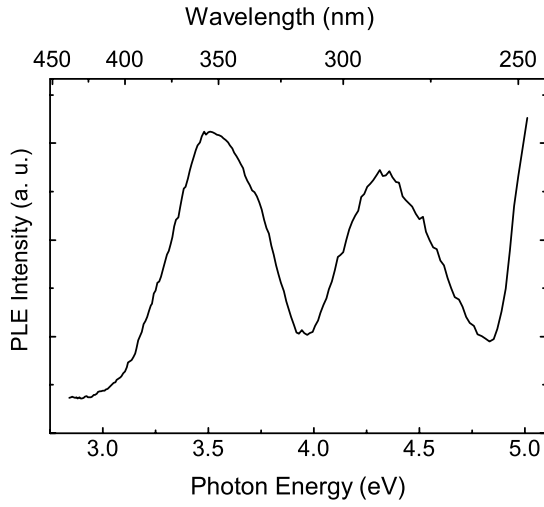


Fig. 3. PLE spectrum of the sample monitored at 2.50 eV.

to the continuum states of a-Si NPs, while that around 4.30 eV is due to the silicon nitride matrix surrounding a-Si NPs. It is noteworthy that the PL band of a-Si NPs with respect to the PLE excitation band also has a large Stokes shift about 1 eV. This observation implies that the PL suffers carriers diffusion and energy relaxation processes before radiative recombination. That is to say, the photogenerated carriers may be generated mostly in the quantized levels of the a-Si NPs and then transferred to the surface localized states in which the carriers recombine through an excitonic process.

Many experimental and theoretical works have shown that the interface states induced by structural or compositional disorders play a rather crucial role in determining the PL behavior of Si NPs composite structures [14,15]. These surface localized defects and disorder compose the shallow states which contribute to part of exponential tail and sub band of the optical absorption. It is believed that such surface states, for example the single covalent Si-Si bonds, can serve as the traps and recombination centers [16]. Figure 4 shows the optical absorption spectrum of the sample. For comparison, the PL spectrum obtained under 325 nm He-Cd laser excitation is also shown. It can be seen that the main peak of the PL spectrum has a significant redshift compared with the exponential tail absorption edge which associates with the transitions between the extended states and band-tail states. Such a behavior indicates that the radiative combination of the photogenerated carriers take place between shallow trap states of electrons and holes rather than the quantized states.

In the Si-in-SiN_x compound film, it is believed that the luminescence originates from the radiative recombination of excitons trapped in the surface states. The isolated spherical Si NPs are embedded in the silicon nitride matrix. Each Si particle is wrapped by the hydrogen-rich amorphous silicon nitride grain-boundary layer. The carriers generate mostly in the Si NPs, and then diffuse to

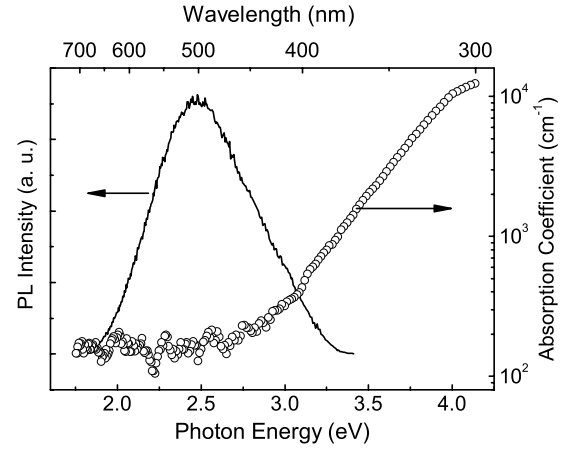


Fig. 4. PL and absorption spectra of the sample.

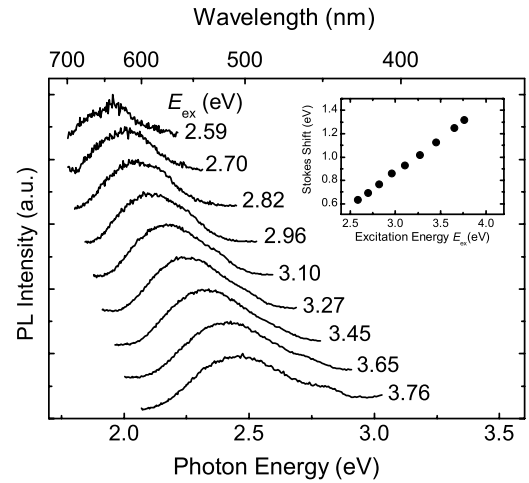


Fig. 5. PL spectra of the sample at different E_{ex} . The inset shows the dependence of the Stokes shift on E_{ex} .

the surrounding grain-boundary. Meanwhile, part of carriers generated in the silicon nitride matrix also can diffuse to the grain-boundary layers. Because the isolated Si NPs have a much larger capture radius than that of the dangling bond defects [17], the isolated Si NPs embedded in silicon nitride matrix favor the trap of photogenerated carriers. The isolated Si NPs tend to act as the radiative recombination centers of photogenerated carriers, and hence suppress the nonradiative recombination in the silicon nitride matrix.

In order to understand the PL mechanism clearly, the PL spectra taken under different E_{ex} were measured as shown in Figure 5. As can be seen, both the PL peak energy and their FWHM show a decrease trend with decreasing the E_{ex} , and no obvious PL can be observed when the E_{ex} lower than 2.50 eV. It is also observed that the Stokes shift between PL and excitation dramatically decreases with the E_{ex} , as shown in the inset of Figure 5. These behaviors can be interpreted based on the surface

excitonic radiative recombination model combining with an assumption of there being a size distribution of a-Si NPs. The a-Si NPs in the investigated film usually have a size distribution as a consequence of the fluctuation of experimental conditions, from which the PL would show a broad PL band as shown in Figure 1. Since the band gap of a-Si nanoparticle increases with the decrease in their size due to quantum confinement effect, the carriers in smaller a-Si NPs cannot be excited when the excitation energy is lower than their band gap. As a result, the PL peak energy would behave in a continuous redshift with decreasing the E_{ex} , and their FWHM monotonic diminishes as well. When the E_{ex} is lower than 2.50 eV, the vanishment of the PL should be the result of no large enough a-Si NPs being excited. The Stokes shift between PL and excitation is the result of carriers thermalizing at surface states which are related to interface bonding configurations and strains of the a-Si NPs. For smaller a-Si NPs, previous investigations have shown that together with the band gap widening due to quantum confinement effect, the reduction in their radius would make the bonding configurations at their surface more disordered and strained, which can cause a significant enlargement of the Stokes shift.

4 Conclusions

In conclusion, we have investigated the PL characteristics of the Si-in-SiN_x compound film. The PL and PLE results show that both the a-Si NPs and the silicon nitride matrix are active in the generation process of carriers. In conjunction with the PL characteristics and the absorption properties, we can conclude that the luminescence of the a-Si NPs composite structure originates from the radiative recombination of the excitons trapped in the surface states. The surface passivation and chemical surroundings of Si NPs have a significant influence on the PL of the a-Si NPs composite structure.

This work was supported by Grants (Nos. E2004000119 and E2006000999) from Natural Foundation of Hebei Province, P.R. China.

References

1. L.T. Canham, Appl. Phys. Lett. **57**, 1046 (1990)
2. B. Delley, E.F. Steigmeier, Appl. Phys. Lett. **67**, 2370 (1995)
3. L. Pavesi, L.D. Negro, C. Mazzoleni, G. Franzo, F. Priolo, Nature **408**, 440 (2000)
4. W.L. Ng, M.A. Lourenco, R.M. Gwilliam, S. Ledain, G. Shao, K.P. Homewood, Nature **410**, 192 (2001)
5. Z. Pei, Y.R. Chang, H.L. Hwang, Appl. Phys. Lett. **80**, 2839 (2002)
6. J.H. Kim, K.A. Jeon, S.Y. Lee, J. Appl. Phys. **98**, 014303 (2005)
7. L.B. Ma, R. Song, Y.M. Miao, C.R. Li, Y.Q. Wang, Z.X. Cao, Appl. Phys. Lett. **88**, 093102 (2006)
8. M.S. Yang, K.S. Cho, J.H. Jhe, S.Y. Seo, J.H. Shin, K.J. Kim, D.W. Moon, Appl. Phys. Lett. **85**, 3408 (2004)
9. N.M. Park, C.J. Choi, T.Y. Seong, S.J. Park, Phys. Rev. Lett. **86**, 1355 (2001)
10. W. Yu, W.B. Lu, L. Han, G.S. Fu, J. Phys. D: Appl. Phys. **37**, 3304 (2004)
11. G.S. Fu, Y.B. Yang, W. Yu, W.B. Lu, W.G. Ding, L. Han, Int. J. Mod. Phys. B **19**, 2704 (2005)
12. T. Noma, K.S. Seol, H. Kato, M. Fujimaki, Y. Ohki, Appl. Phys. Lett. **79**, 1995 (2001)
13. H. Kato, N. Kashio, Y. Ohki, K.S. Seol, T. Noma, J. Appl. Phys. **93**, 239 (2003)
14. A. Puzder, A.J. Williamson, J.C. Grossman, G. Galli, Phys. Rev. Lett. **88**, 097401 (2002)
15. G. Hadjisavvas, P.C. Kelires, Phys. Rev. Lett. **93**, 226104 (2004)
16. G. Allan, C. Delerue, M. Lannoo, Phys. Rev. Lett. **76**, 2961 (1996)
17. T. Kamei, P. Stradins, A. Matsuda, Appl. Phys. Lett. **74**, 1707 (1999)